Nonlinearities in the harmonic spectrum of heavy ion collisions with ideal and viscous hydrodynamics

D. Teaney* and L. Yan†

Department of Physics and Astronomy, Stony Brook University, Stony Brook, New York 11794, USA

(Received 24 August 2012; published 31 October 2012)

We determine the nonlinear hydrodynamic response to geometrical fluctuations in heavy ion collisions using ideal and viscous hydrodynamics. This response is characterized with a set of nonlinear response coefficients that determine, for example, the v_5 that is produced by an ϵ_2 and an ϵ_3. We analyze how viscosity damps both the linear and nonlinear response coefficients, and provide an analytical estimate that qualitatively explains most of the trends observed in more complete simulations. Subsequently, we use these nonlinear response coefficients to determine the linear and nonlinear contributions to v_1, v_4, and v_5. For viscous hydrodynamics the nonlinear contribution is dominant for v_4, v_5, and higher harmonics. For v_1, the nonlinear response constitutes an important $\sim$25% correction in midcentral collisions. The nonlinear response is also analyzed as a function of transverse momentum for v_1, v_4, and v_5. Finally, recent measurements of correlations between event planes of different harmonic orders are discussed in the context of nonlinear response.

DOI: 10.1103/PhysRevC.86.044908 PACS number(s): 25.75.Gz, 21.65.−f, 24.10.Nz, 47.75.+f

I. INTRODUCTION

The goal of the BNL Relativistic Heavy Ion Collider (RHIC) and the CERN Large Hadron Collider (LHC) heavy ion programs is to produce and to characterize the quark gluon plasma (QGP), a prototype for non-Abelian plasmas. One of the best ways to understand the transport properties of the experimentally produced plasma is through anisotropic flow [1–3]. In a heavy ion collision the nuclei pass through each other, and the resulting energy density in the transverse plane fluctuates in coordinate space from event to event. If the mean free path is short compared to the system size, the produced plasma will respond as a fluid to the pressure gradients and convert these coordinate space fluctuations to long range momentum space correlations between the produced particles. In the last two years it was gradually realized [4–6] that all of the long range momentum-space correlations known colloquially as the "ridge" and "the Mach cone" are manifestations of this collective flow [7,8]. This realization gave rise to a large variety of flow observables which provide an unprecedented experimental check of the overall correctness of the hydrodynamic picture of heavy ion events [7,9–11]. Further, different observables have different sensitivity to the shear viscosity of the plasma [12], and therefore a global analysis of flow can provide cross-correlated constraints on η/s.

One of the most direct measurements is the harmonic spectrum of the produced particles. The final state momentum spectrum for each event can be expanded in harmonics

$$\frac{dN}{d\phi_{\boldsymbol{p}}} = \frac{N}{2\pi}\left(1 + 2\sum_{n=1}^{\infty} v_n \cos(n\phi_{\boldsymbol{p}} - n\Psi_n)\right), \quad (1.1)$$

where $\phi_{\boldsymbol{p}}$ is the azimuthal angle of the produced particles and Ψ_n is the event plane angle.[1] The averaged square of these harmonics, i.e., $\langle\langle v_n^2\rangle\rangle$, can be measured experimentally by studying two particle correlations [1]. There is strong experimental and theoretical evidence that the harmonic coefficients, v_2 and v_3, are to a good approximation linearly proportional to the deformations in the initial energy density in the transverse plane. For example, the experimental ratio $\langle\langle v_3^2\rangle\rangle/\langle\langle v_2^2\rangle\rangle$ closely follows the geometric deformations $\langle\langle \epsilon_3^2\rangle\rangle/\langle\langle \epsilon_2^2\rangle\rangle$ as a function of centrality [7]. Event-by-event simulations with ideal hydrodynamics reproduce this trend, and show that the event plane angles Ψ_2 and Ψ_3 are strongly correlated with the angles of the initial deformations [13].

However, in an insightful paper Gardim *et al.* [14] studied the correlation between higher harmonics, v_4 and v_5, and the initial spatial deformations within ideal hydrodynamics. This work explained and quantified the extent to which the higher harmonics such as v_4 and v_5 arise predominantly from the nonlinearities of the medium response. For example, for midcentral collisions the observed v_5 is predominantly a result of the interactions between v_2 and v_3. This work was motivated in part by previous event-by-event simulations by Heinz and Qiu [13] which showed that Ψ_4 and Ψ_5 are uncorrelated with the fourth and fifth harmonics of the spatial deformation. Based on the centrality dependence of this decorrelation, these authors anticipated (but did not quantify) the importance of v_2-v_3 mode-mixing in determining v_5.

The goal of this work is to systematically characterize the nonlinear response of the medium. First, in Sec. II we introduce a set of nonlinear response coefficients, and describe how these coefficients can be used in conjunction with a Glauber model to determine $\langle\langle v_n^2\rangle\rangle$. The strongest nonlinear response stems from the interactions between v_2 and the other harmonics, and consequently a prominent response coefficient is $w_{5(23)}/\epsilon_2\epsilon_3$,

*derek.teaney@stonybrook.edu
†li.yan@stonybrook.edu

[1] Following tradition, we have expanded the particle distribution in terms of cosines and phases Ψ_n rather than cosines and sines.

which determines the v_5 produced by an elliptic and triangular deformation. In Sec. III B we determine these response coefficients using both ideal and viscous hydrodynamics, and study how the response depends on the shear viscosity. With these nonlinear coefficients, together with the linear response, we make several predictions for v_1, v_4, and v_5 in ideal and viscous hydrodynamics in Sec. IV. Finally, in Sec. IV we also study the transverse momentum dependence of v_1, v_4, and v_5.

In this work we will determine the harmonic spectrum by characterizing the quadratic response of the system to small deformations. Alternatively, one could simply run hydrodynamics event-by-event and compute the averages that are needed to compare to experiment [13,15–19]. While event-by-event hydrodynamics is the best for this pragmatic purpose, the framework of nonlinear response can yield valuable insight into the physics of these rather involved simulations.

II. NONLINEAR RESPONSE

A. The cumulant expansion

In hydrodynamic simulations of heavy ion collisions the medium is first modeled with an initial state model, then the medium is evolved with hydrodynamics, and finally the particle spectrum is computed by making kinetic assumptions about the fluid. The final state particle spectrum for each event can be expanded in harmonics

$$\frac{dN}{d\phi_p} = \frac{N}{2\pi}\left(1+\sum_{n=1}^{\infty} v_n e^{in(\phi_p-\Psi_n)} + \text{c.c.}\right), \qquad (2.1)$$

where here and below c.c. denotes complex conjugation. The root mean squares of v_n are easily determined experimentally, and are given a special notation

$$v_n\{2\} \equiv \sqrt{\langle\langle v_n^2\rangle\rangle}, \qquad (2.2)$$

where $\langle\langle\ldots\rangle\rangle$ denotes the average over events.

In the next sections we will describe how the momentum space response is related to the initial state geometry. To this end, the spatial distribution of the initial entropy density in the transverse plane,

$$\rho(\boldsymbol{x}) \equiv \frac{\tau_0 s(\boldsymbol{x})}{\int d^2x\, \tau_0 s(\boldsymbol{x})}, \qquad (2.3)$$

is quantified with a cumulant expansion [9], where $\boldsymbol{x} = (x, y) = (r\cos\phi, r\sin\phi)$ are the coordinates in the transverse plane and τ_o is the initial Björken time [20]. Specifically the n, m-th moment of the entropy distribution is defined as

$$\rho_{n,m} \equiv \int d^2\boldsymbol{x}\, \rho(\boldsymbol{x})\,(r^2)^{(n-m)/2} r^m e^{im\phi}, \qquad (2.4)$$

where $(n-m)/2$ is a non-negative integer. This moment is closely related to the n, m-th cumulant $W_{n,m}$

$$W_{n,m} \propto \rho_{n,m} - \text{contractions}. \qquad (2.5)$$

The meaning of Eq. (2.5) will be clarified through examples, with additional details about the cumulant expansion relegated to the literature [9,21]. The radial variation of $\rho(\boldsymbol{x})$ is quantified by the radial cumulants, $\langle r^2\rangle$ and $\langle r^4\rangle - 2\langle r^2\rangle^2$, while the the azimuthal variation of $\rho(\boldsymbol{x})$ is quantified by the azimuthal cumulants

$$\epsilon_1 e^{i\Phi_1} = -\frac{\langle r^3 e^{i\phi}\rangle}{\langle r^3\rangle}, \qquad (2.6)$$

$$\epsilon_2 e^{i2\Phi_2} = -\frac{\langle r^2 e^{i2\phi}\rangle}{\langle r^2\rangle}, \qquad (2.7)$$

$$\epsilon_3 e^{i3\Phi_3} = -\frac{\langle r^3 e^{i3\phi}\rangle}{\langle r^3\rangle}. \qquad (2.8)$$

Here $\langle\ldots\rangle$ denote an average over $\rho(\boldsymbol{x})$ for a single event, and Φ_1, Φ_2, and Φ_3 are the participant plane angles. These coordinate space angles are distinct from the momentum space angles Ψ_1, Ψ_2, and Ψ_3.

For the lowest harmonics the azimuthal cumulants and the azimuthal moments coincide, and these definitions will appear obvious to most readers. For the fourth harmonic and higher, we will depart from traditional moment based definition, and quantify the deformations with cumulants rather than moments[2]

$$\mathcal{C}_4 e^{i4\Phi_4} \equiv -\frac{1}{\langle r^4\rangle}[\langle r^4 e^{i4\phi}\rangle - 3\langle r^2 e^{i2\phi}\rangle^2]. \qquad (2.9)$$

The motivation for this definition can be seen by studying an elliptic Gaussian distribution,

$$\rho(\boldsymbol{x}) = \frac{1}{2\pi\sigma_x\sigma_y} e^{-\frac{x^2}{2\sigma_x^2}-\frac{y^2}{2\sigma_y^2}}, \qquad (2.10)$$

which has $\mathcal{C}_4 = 0$, although ϵ_4 is nonzero and is of order ϵ_2^2. Similarly we define

$$\mathcal{C}_5 e^{i5\Phi_5} \equiv -\frac{1}{\langle r^5\rangle}[\langle r^5 e^{i5\phi}\rangle - 10\langle r^2 e^{i2\phi}\rangle\langle r^3 e^{i3\phi}\rangle] \qquad (2.11)$$

and remark that a Gaussian distribution deformed by an ϵ_3,

$$s(\boldsymbol{x},\tau) \propto \left[1 + \frac{\langle r^3\rangle\epsilon_3}{24}\left(\left(\frac{\partial}{\partial x}\right)^3 - 3\left(\frac{\partial}{\partial y}\right)^2\frac{\partial}{\partial x}\right)\right] e^{-\frac{x^2}{2\sigma_x^2}-\frac{y^2}{2\sigma_y^2}}, \qquad (2.12)$$

has $\mathcal{C}_5 = 0$, although $\langle r^5 e^{i5\phi_s}\rangle$ is nonzero and of order $\epsilon_2\epsilon_3$.

We will characterize the hydrodynamic response to the cumulants defined above in the next section.

B. Nonlinear response to the cumulants

We expect the response of the system to be dominated by the lowest cumulants. Motivated by Fourier analysis [9], we replace the general distribution $\rho(\boldsymbol{x})$ with a Gaussian, Eq. (2.10), whose second moments have been adjusted to reproduce $\langle r^2\rangle = \sigma_x^2 + \sigma_y^2$ and $\epsilon_2 = (\sigma_y^2 - \sigma_x^2)/(\sigma_x^2 + \sigma_y^2)$. In Ref. [9] we showed that a Gaussian + forth order cumulants reproduces the results of smooth Glauber initial conditions in detail. If a Gaussian with a non-negligible ϵ_2 is simulated, the

[2]For $n \geqslant 4$ we notate the cumulant based eccentricity by $\mathcal{C}_n$ to differentiate this quantity from the moment based eccentricity ϵ_n. $\mathcal{C}_n$ is equal to $W_{n,n}$ up to normalization and an overall factor of $\langle r^n\rangle$.

particle spectrum produced by this background contains all even harmonics

$$\frac{dN}{d\phi_p} = \frac{N}{2\pi}\,(1 + w_2 e^{i2(\phi_p-\Phi_2)} + w_{4(22)} e^{i4(\phi_p-\Phi_2)} + \cdots + \text{c.c.}). \tag{2.13}$$

For small ϵ_2 the response coefficient w_2 describes the linear response to the deformation and is proportional to ϵ_2, while $w_{4(22)}$ describes the nonlinear response and is proportional to ϵ_2^2. Below, we will assume that ϵ_2 is small enough that this scaling with ϵ_2 applies. Further, we have truncated the expansion in Eq. (2.13) at quadratic order in ϵ_2, and will continue to do this implicitly from now on. The working assumption in this paper is that the most important nonlinearity stems from the almond shape of the background.

If the Gaussian distribution is perturbed by a small fourth-order cumulant $\mathcal{C}_4 e^{i4\Phi_4}$, then the resulting particle spectra will be described by

$$\frac{dN}{d\phi_p} = \frac{N}{2\pi}(1 + w_2 e^{i2(\phi_p-\Phi_2)} + w_4 e^{i4(\phi_p-\Phi_4)} + w_{4(22)} e^{i4(\phi_p-\Phi_2)} + \text{c.c.})\,, \tag{2.14}$$

where w_4 captures the linear response to the fourth-order cumulant and is proportional to $\mathcal{C}_4$ for small $\mathcal{C}_4$. In writing Eq. (2.14) we have neglected terms proportional to $\mathcal{C}_4\epsilon_2$, which can contribute to v_2 and reduce the perfect correlation between Ψ_2 and Φ_2. Comparing Eq. (2.14) with the definition of v_4, Eq. (2.1), we see that v_4 is determined by the linear and quadratic response

$$v_4 e^{-i4\Psi_4} = w_4 e^{-i4\Phi_4} + w_{4(22)} e^{-i4\Phi_2}\,. \tag{2.15}$$

Squaring this result and averaging over events we see that

$$v_4\{2\} \equiv \langle\langle v_4^2\rangle\rangle^{1/2} = \langle\langle |w_4 e^{-i4\Phi_4} + w_{4(22)} e^{-i4\Phi_2}|^2\rangle\rangle^{1/2}\,. \tag{2.16}$$

In writing Eq. (2.14) we have neglected the nonlinear contributions of ϵ_1 and ϵ_3 to v_4 since v_3 and v_1 are small compared to v_2 for midperipheral collisions.

Similarly, if the Gaussian background distribution is perturbed by a third order cumulant and a fifth-order cumulant $\mathcal{C}_5$, then v_5 is determined by a combination of the linear and nonlinear response. The response to $\mathcal{C}_5$ is small [12], and therefore we will neglect the nonlinearities due to $\epsilon_2\mathcal{C}_5$, but we will keep the nonlinearities due to $\epsilon_2\epsilon_3$. With this approximation scheme the particle spectrum through quadratic order reads

$$\frac{dN}{d\phi_p} = \frac{N}{2\pi}\,(1 + w_3 e^{i3(\phi_p-\Phi_3)} + w_5 e^{i5(\phi_p-\Phi_5)} + w_{1(23)} e^{i\phi_p - 3\Phi_3 + 2\Phi_2} + w_{5(23)} e^{i5\phi_p - 3\Phi_3 - 2\Phi_2} + \text{even harmonics} + \text{c.c})\,. \tag{2.17}$$

Comparing this equation to the definition of v_5, we see that

$$v_5\{2\} = \langle\langle |w_5 e^{-i5\Phi_5} + w_{5(23)} e^{-i(3\Phi_3+2\Phi_2)}|^2\rangle\rangle^{1/2}, \tag{2.18}$$

which is clearly analogous with v_4 case. Finally, if the distribution has a net dipole asymmetry ϵ_1, then v_1 is given a combination of the linear and nonlinear response

$$v_1\{2\} = \langle\langle |w_1 e^{-i\Phi_1} + w_{1(23)} e^{-i(3\Phi_3-2\Phi_2)}|^2\rangle\rangle^{1/2}, \tag{2.19}$$

where w_1 notates the linear response to ϵ_1. In writing this result for v_1 we have neglected the nonlinear interaction between v_1 and v_2, i.e., $w_{1(21)}$. Thus Eq. (2.19) makes the simplifying assumption that v_1 is small compared to v_3, while a more complete treatment would include a $w_{1(21)}$ contribution.

Let us discuss how this formalism can be used to study the p_T dependence of the flow. The particle spectra is expanded in harmonics

$$\frac{\mathrm{d}N}{\mathrm{d}p_T\mathrm{d}\phi_p} \equiv \frac{\mathrm{d}N}{\mathrm{d}p_T}\left(1 + \sum_{n=1}^{\infty} v_n(p_T) e^{in(\phi_p - \Psi_n(p_T))} + \text{c.c.}\right), \tag{2.20}$$

where the phase, $\Psi_n(p_T)$, is in general a function of p_T. Then $v_n(p_T)\{2\}$ in the Ψ_n plane is normally defined as

$$v_n(p_T)\{2\} \equiv \begin{cases} \frac{\langle\langle v_n(p_T) v_n \cos(n(\Psi_n(p_T)-\Psi_n))\rangle\rangle}{v_n\{2\}} & n > 1 \\ -\frac{\langle\langle v_1(p_T) v_1 \cos(\Psi_1(p_T)-\Psi_1)\rangle\rangle}{v_1\{2\}} & n = 1 \end{cases}, \tag{2.21}$$

where we have inserted an extra minus sign for $v_1(p_T)$, since the integrated v_1 is negative. The phase angle $\Psi_n(p_T)$ is often assumed to equal Ψ_n. Using the formalism outlined above we write $v_1(p_T)$ as a sum of the linear and nonlinear response

$$v_1(p_T) e^{-i\Psi_1(p_T)} = w_1(p_T) e^{-i\Phi_1} + w_{1(23)}(p_T) e^{-i3\Phi_3 + i2\Phi_2}\,. \tag{2.22}$$

Then the numerator of $v_1(p_T)\{2\}$ is given by

$$\begin{aligned} &\langle\langle v_1(p_T) v_1 \cos(\Psi_1(p_T) - \Psi_1)\rangle\rangle \\ &= \langle\langle w_1(p_T) w_1 + w_{1(23)}(p_T) w_{1(23)} + [w_1(p_T) w_{1(23)} \\ &\quad + w_{1(23)}(p_T) w_1] \cos(\Phi_1 - 3\Phi_3 + 2\Phi_2)\rangle\rangle\,, \end{aligned} \tag{2.23}$$

and the denominator is given by the integrated expression for $v_1\{2\}$, Eq. (2.19). Similar expressions follow for $v_4(p_T)$ and $v_5(p_T)$.

Finally, let us place some older measurements and calculations of $v_4(p_T)$ into context [22–28]. Traditionally, what was referred to as $v_4(p_T)$ would today be called $v_4(p_T)$ in the Ψ_2 plane:

$$v_{4(22)}(p_T)\{2\} \equiv \frac{\langle\langle v_4(p_T) v_2 \cos(4\Psi_4(p_T) - 2\Psi_2 - 2\Psi_2)\rangle\rangle}{v_2\{2\}}\,. \tag{2.24}$$

As discussed in the conclusions, the differences between $v_{4(22)}(p_T)\{2\}$ and $v_4(p_T)\{2\}$ can be used to partially disentangle the linear and nonlinear response.

C. Summary

The goal of the present work is to compute the linear and nonlinear response coefficients, and to use these coefficients together with an initial state model to determine $\langle\langle v_n^2\rangle\rangle$ with Eqs. (2.16), (2.18), and (2.19). For v_5 the step by step procedure is: (i) use hydrodynamics to determine the response coefficients

$$\frac{w_5}{\mathcal{C}_5} \quad \text{and} \quad \frac{w_{5(23)}}{\epsilon_2\epsilon_3}, \tag{2.25}$$

for vanishingly small $\mathcal{C}_5$ and $\epsilon_2\epsilon_3$; (ii) use the initial state model to determine the geometric coefficients that are needed in Eq. (2.18), $\langle\langle\mathcal{C}_5^2\rangle\rangle$, $\langle\langle(\epsilon_2\epsilon_3)^2\rangle\rangle$, and $\langle\langle\mathcal{C}_5\epsilon_2\epsilon_3\cos(5\Phi_5-3\Phi_3-2\Phi_2)\rangle\rangle$; (iii) combine these results in Eq. (2.18) to determine the complete hydrodynamic prediction for $\langle\langle v_5^2\rangle\rangle$. For the initial state model we have adopted the Phobos Monte Carlo Glauber model [29] and taken the entropy density proportional to the transverse density of wounded nucleons in the xy plane. When computing $\langle r^5e^{i5\phi}\rangle$ and $\langle r^5\rangle$, for example, we have treated the wounded nucleons as points in the transverse plane. We note that there is a very strong geometric correlation between participant planes differing by two, e.g.,

$$\langle\langle\mathcal{C}_5\epsilon_2\epsilon_3e^{i(5\Phi_5-3\Phi_3-2\Phi_2)}\rangle\rangle \quad \text{and} \quad \langle\langle\epsilon_1\epsilon_2\epsilon_3e^{i(3\Phi_3-\Phi_1-2\Phi_2)}\rangle\rangle. \tag{2.26}$$

This geometric correlation can be studied analytically in an independent source model [30], and is easily attributed to the elliptic shape of the overlap region [9,30,31].

III. HYDRODYNAMIC SIMULATIONS

A. Ideal and viscous hydrodynamics

To calculate the nonlinear response we use a hydrodynamics code that implements conformal second-order hydrodynamics [32]. The numerical scheme is based on a central scheme developed and tested in Ref. [33], although the equations of motion for the π^{ij} are somewhat different from what was studied in that work.[3] η/s is held constant, and the ratio of second-order hydro parameters are taken from their AdS/CFT values [32,34], e.g., $\tau_\pi/(\eta/sT) = 4-2\ln 2$. The equation of state partially parametrizes lattice results and was used previously by Romatschke and Luzum [35]. Finally, we have followed the time "honored" constant temperature freeze-out prescription, with $T_{\rm fo} = 150\,\text{MeV}$. For simplicity we have adopted the popular quadratic ansatz for the viscous correction to the thermal distribution function [2]

$$f(P) = f_o(P) + \delta f(P), \quad \delta f(P) \equiv \frac{f_o(1\pm f_o)}{2(e+\mathcal{P})T^2}P^\mu P^\nu\pi_{\mu\nu}, \tag{3.1}$$

where $f_o(P) = 1/(\exp(-P\cdot U(X)/T)\mp 1)$ is the equilibrium distribution, $e+\mathcal{P}$ is the enthalpy, and δf is the first viscous correction [2,36]. Although we have used the quadratic ansatz in this work, a linear ansatz is probably more appropriate for QCD-like theories and can effect the integrated flow for the higher harmonics [25,37].

For the simulations shown below we have followed the centrality classification given in Ref. [13] which is documented in Table I. of that work. Our procedure to determine the response coefficient at a given impact parameter largely follows Ref. [9], which should be referred to for additional details—see especially Appendix A of that work. Briefly, for each impact parameter we determine the average squared radius $\langle r^2\rangle$, and initialize a Gaussian distribution that is deformed by the appropriate cumulant. The Gaussian is normalized to reproduce the total entropy in the event. For instance, to determine the $w_{5(23)}$ we initialize the distribution given in Eq. (2.12) with $\epsilon_2 = \epsilon_3 = 0.02$. A technical complication is that the distribution in Eq. (2.12) must be regulated [9], and the regularization procedure introduces a small $\mathcal{C}_5$. However, the spurious $\mathcal{C}_5$ decreases faster than ϵ^3 and can be made arbitrarily small compared to the signal. Empirically we find that the spurious $\mathcal{C}_5$ decreases approximately as ϵ^5, and the v_5 from the spurious cumulant is negligibly small compared to the v_5 from the $\epsilon_2\epsilon_3$ combination.

TABLE I. The geometrical ratios in Eq. (4.6) as a function of centrality.

Centrality %	2.5	7.5	12.5	17.5	25.0	35.0	45.0	55.5
$\sqrt{\langle\epsilon_2^4\rangle/\langle\epsilon_2^2\rangle^2}$	1.40	1.33	1.26	1.22	1.20	1.18	1.17	1.16
$\sqrt{\langle(\epsilon_2\epsilon_3)^2\rangle/(\langle\epsilon_2^2\rangle\langle\epsilon_3^2\rangle)}$	0.99	0.97	0.96	0.95	0.94	0.93	0.930	0.92
$\sqrt{\langle\epsilon_2^2\rangle/\langle\epsilon_1^2\rangle}$	2.12	2.78	3.22	3.46	3.56	3.40	3.04	2.64

B. The nonlinear response coefficients in ideal and viscous hydrodynamics

In this section we will study the nonlinear response coefficients systematically. In particular we study how the linear and nonlinear response coefficients depend on (i) transverse momentum, (ii) centrality, and (iii) shear viscosity.

1. Momentum dependence of the response coefficients

Figure 1 examines the p_T dependence of the linear and nonlinear response coefficients, w_4 and $w_{4(22)}$, which are characteristic of the response coefficients more generally. First, focus on the ideal curves in Figs. 1(a) and 1(b).

At large p_T the nonlinear response curves show a characteristic quadratic rise with p_T, while the linear response curves show a characteristic linear rise. This difference between the nonlinear and linear response is known from previous studies of v_4 [23]. Later, when examining nonlinear corrections to v_1 (see Fig. 6), we will see that the nonlinear corrections are most important at high p_T and exhibit a characteristic quadratic rise. Comparing Figs. 1(a) and 1(b), we see that viscous corrections are smaller for the nonlinear response $w_{4(22)}(p_T)/\epsilon_2^2$, than for the linear response $w_4(p_T)/\mathcal{C}_4$. This is a generic result as will be discussed in detail in Sec. III B3.

We also note that the linear response curves shown in Fig. 1(a) change sign for sufficiently large viscosity. This is an artifact of the first viscous correction, δf, and the quadratic ansatz. To see this, we have plotted $w_4(p_T)$ and and $w_{4(22)}(p_T)$ using only the unmodified distribution function f_o in Figs. 1(a)

[3]However, when additional nonconformal second order gradients are added to our equations of motion and the parameters are matched, our current numerical can be compared directly to Ref. [33]. If this is done, the two hydrocodes yield the same answers to 0.1% for the type of problems considered in this work.

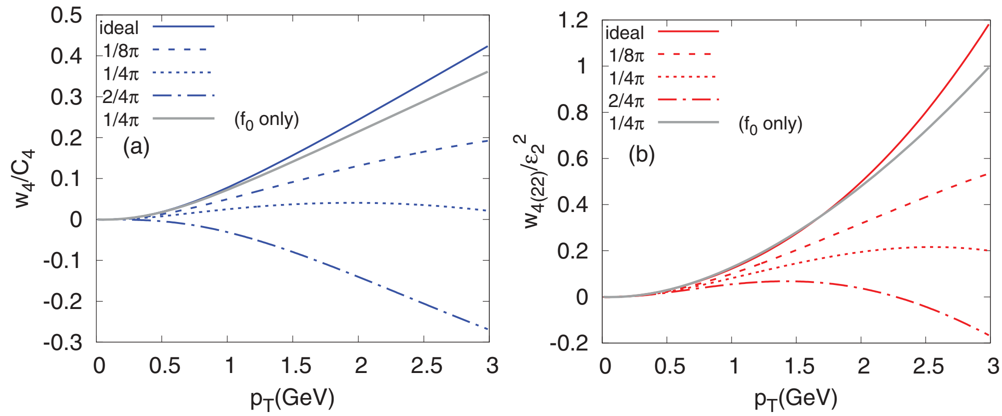

FIG. 1. (Color online) The linear and nonlinear response coefficients for v_4, $w_4(p_T)$, and $w_{4(22)}(p_T)$, for ideal and viscous hydrodynamics. The grey curves (which are shown only for $\eta/s = 1/4\pi$) exhibit the resulting response when the equilibrium distribution f_o is used, and the viscous correction, δf, is neglected [see Eq. (3.1)].

and 1(b). For large viscosity the δf correction to v_4 and v_5 is not small compared to the ideal contribution f_o, and this causes a reduction of the response, which is more pronounced for the higher harmonics, v_4 and v_5. In full kinetic theory calculations $w_4/\mathcal{C}_4$ and $w_5/\mathcal{C}_5$ remain positive and approach zero as the viscosity is increased [12]. Thus, the negative $w_4/\mathcal{C}_4$ indicates that the first viscous correction has become too large to be trusted. Below, we will simply set the response coefficients to zero when this is the case. Experience with kinetic theory suggests that this ad hoc procedure is not far from what really happens.

2. Centrality dependence of the response coefficients

Figure 2 shows the linear and nonlinear response coefficients in ideal and viscous hydrodynamics. There are several salient features contained in these plots. First, note that the magnitude of the linear response coefficient $w_5/\mathcal{C}_5$ is quite small in the viscous case, and $w_5/\mathcal{C}_5$ has been multiplied by ten to make the curves visible. The nonlinear response $w_{5(23)}$ coefficient is significantly larger. The implications of this difference will be studied in the next section when we multiply the response coefficients by $\mathcal{C}_5$ and $\epsilon_2\epsilon_3$ respectively. Second, all of the response coefficients are reduced by viscosity, especially in noncentral collisions.

The viscous $w_4/\mathcal{C}_4$ and $w_5/\mathcal{C}_5$ curves stop abruptly as a function of centrality, since we have truncated the curves when response falls below zero. As discussed above (see Fig. 1), this is because viscous corrections to the thermal distribution function (δf) become larger for more peripheral collisions, and this correction is magnified by the high harmonic number. We have therefore truncated the w_4 and w_5 response curves when the response turns negative. At this point δf constitutes an order one correction and can no longer be trusted.

3. Dependence on viscosity

It is interesting to note that viscous reduction for w_1/ϵ_1 is smaller than for $w_4/\mathcal{C}_4$ and $w_5/\mathcal{C}_5$. This pattern of viscous corrections for linearized perturbations is studied further in Fig. 3(a). Each linearized perturbation labeled by n, m-th cumulant is damped by a factor $\sim \exp(-\Gamma_{n,m}\,\tau_{\rm final})$ relative to ideal hydrodynamics, where $\tau_{\rm final}$ is an estimate for the duration of the event. Analytical work shows that the damping coefficients $\Gamma_{n,m}$ scale as

$$\Gamma_{n,m}\,\tau_{\rm final} \sim \frac{\ell_{\rm mfp}}{L}\left(\frac{n-m}{2}+m\right)^2, \tag{3.2}$$

for a conformal equation of state and a particular background flow [21]. Thus, each power of r^2 and each harmonic order in Eq. (2.4) increases $(n-m)/2+m$ by one unit. Our numerical work [Fig. 3(a)] is not limited to the conformal equation of state or the particular background flow of Ref. [21], and shows that this scaling is reasonably generic [12,38]. Specifically, the formal estimate given in Eq. (3.2) implies a definite pattern among the viscous corrections to v_n:

$$\begin{aligned} -\frac{\Delta w_1}{w_1^{\rm id}} \simeq -\frac{\Delta w_2}{w_2^{\rm id}} \propto 4\,\frac{\eta}{s}, \quad -\frac{\Delta w_3}{w_3^{\rm id}} \propto 9\,\frac{\eta}{s}, \\ -\frac{\Delta w_4}{w_4^{\rm id}} \propto 16\,\frac{\eta}{s}, \quad -\frac{\Delta w_5}{w_5^{\rm id}} \propto 25\,\frac{\eta}{s}, \end{aligned} \tag{3.3}$$

where $\Delta w = w^{\rm viscous} - w^{\rm ideal}$, and $w^{\rm id}$ is the ideal hydro response coefficient. Note, in particular, that the viscous corrections v_1 and v_2 are similar since v_1 and v_2 respond to the dipole asymmetry, $W_{3,1}$, and the ellipticity, $W_{2,2}$, respectively [38]. Since the slopes of the $v_1 : v_2 : v_3 : v_4 : v_5$ curves in Fig. 3(a) have approximately the expected ratios $4 : 4 : 9 : 16 : 25$, our numerical work qualitatively confirms this pattern of viscous corrections.

Figure 3(b) compares the damping rate for the nonlinear response coefficients to the corresponding linear response coefficients. Take $w_{5(23)}$ for example. Since $w_{5(23)}$ is of order $v_2 v_3$ we expect the damping of this nonlinear perturbation to scale as $\sim e^{-\Gamma_{2,2}\tau}e^{-\Gamma_{3,3}\tau}$, and thus the damping rate $\Gamma_{5(23)}$ is expected to scale as

$$\Gamma_{5(23)} \sim \Gamma_{2,2} + \Gamma_{3,3}\,. \tag{3.4}$$

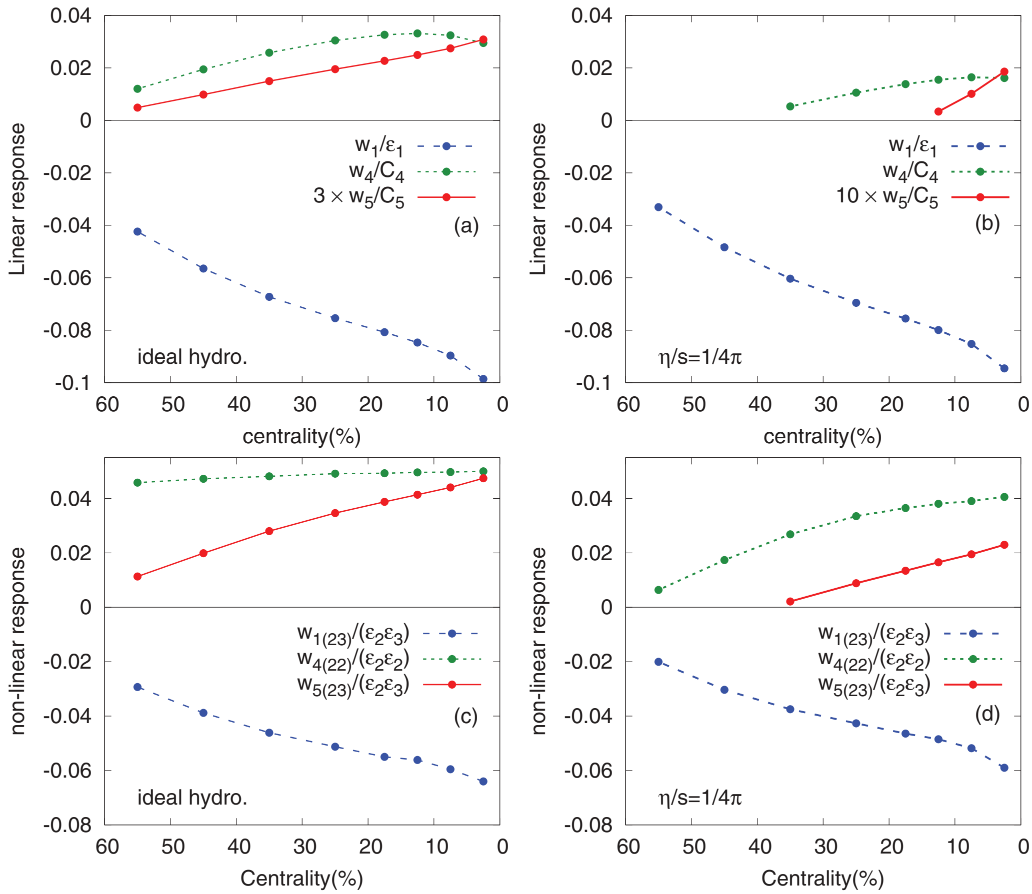

FIG. 2. (Color online) The linear and nonlinear response coefficients for ideal and viscous hydro. In the viscous case the curves are truncated when the response coefficients turn negative, i.e., outside of the regime of validity of viscous hydro.

Thus, we expect the nonlinear and linear response coefficients for v_5 to scale as

$$-\frac{\Delta w_{5(23)}}{w^{\rm id}_{5(23)}} \propto 13\frac{\eta}{s}\,, \qquad -\frac{\Delta w_5}{w^{\rm id}_5} \propto 25\frac{\eta}{s}\,. \tag{3.5}$$

Comparing the slopes of the nonlinear and linear response curves in Fig. 3(b), we see that the slope of the $\Delta w_{5(23)}/w^{\rm id}_{5(23)}$ curve is approximately half of the corresponding $\Delta w_5/w^{\rm id}_5$, and is qualitatively consistent with our heuristic estimate of 13/25. $w_{4(22)}$ and w_4 show a similar pattern of viscous corrections. Finally our estimates seem only partially applicable to v_1. For instance, the reasoning of Eq. (3.4) predicts that the nonlinear damping rates, $\Gamma_{1(23)}$ and $\Gamma_{5(23)}$, should be equal. However, the slope of $\Delta w_{1(23)}/w^{\rm id}_{1(23)}$ is significantly smaller than the $\Delta w_{5(23)}/w^{\rm id}_{5(23)}$, and contradicts this reasoning. Clearly, the nonlinear viscous damping of v_1 is a special case which will have to be investigated more completely at a later date.

IV. RESULTS AND DISCUSSION

A. Results

Having clarified the nonlinear hydrodynamic response, we study the phenomenological implications of these response coefficients. Figure 4 shows v_1, v_4, and v_5 including the linear and nonlinear response as outlined in Sec. II, and is the principal result of this work.

Examining this figures we see that the nonlinear response is an important correction for v_1, and essential for v_4 and v_5. The contribution of the nonlinear response to the total flow increases towards peripheral collisions, and for v_4 and v_5 is of order 50% in midperipheral collisions. This is roughly compatible with simulation results from event-by-event hydrodynamics [13,14]. Especially for viscous hydrodynamics and for v_5, the linear response is negligible in all but the most central bin. Even in the most central bin, the nonlinear contribution to v_5 is about 50% of the total. It is notable, if expected, that for v_1 viscosity reduces the nonlinear contribution relative to the total, while for v_4 and v_5 viscosity increases the nonlinear contributions. This is consistent with the discussion given in Sec. II B.

It will be quite interesting to measure the complete set of event planes $(\Psi_1, \Psi_2, \Psi_3, \Psi_4, \Psi_5)$ and their intercorrelations. These measurements will place a strong experimental constraint on the relative of importance of the nonlinear response [11]. For example, if the nonlinear response is dominant (as implied by the viscous v_5 curves), then a stronger than geometric correlation is expected for certain experimental averages, e.g., $\langle\cos(5\Psi_5 - 3\Psi_3 - 2\Psi_2)\rangle$.

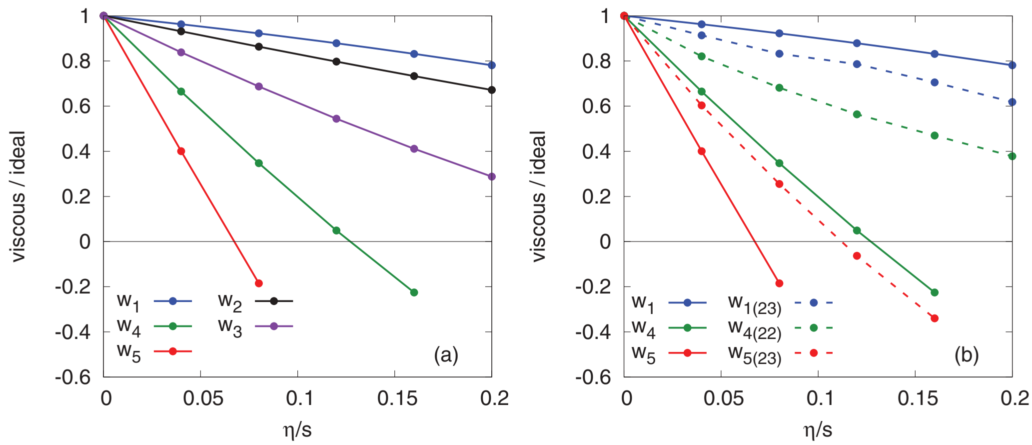

FIG. 3. (Color online) (a) Linear response coefficients w_n as a function of viscosity relative to the ideal response. (b) A comparison of nonlinear and linear response coefficients as a function of viscosity, e.g., $w_{5(23)}$ records the v_5 produces by a combination of ϵ_2 and ϵ_3. The negative values for large viscosity are spurious, and lie beyond the region of applicability of viscous hydrodynamics.

Next we examine the p_T dependence of the v_1, v_4, and v_5. Since v_4 and v_5 are dominated by the nonlinear response we will present our results by scaling v_2^2 and v_2v_3, respectively. Many of the points raised in this and the next paragraph are familiar from earlier studies of v_4 in the Ψ_2 plane. In particular, the importance of nonlinearities and fluctuations in determining the experimental v_4/v_2^2 ratio was understood previously [23,24].

First we note that according to an old argument by Borghini and Ollitrault [23], v_4/v_2^2 should approach $1/2$ at large momentum in ideal hydrodynamics for any given event due to the nonlinearities inherent in the phase space distribution. Their result is easily generalized to v_5, $v_5 = v_2v_3$. The argument follows by computing the freeze-out distribution in a saddle point approximation [39], and can be schematically understood by examining the thermal factor in an approximately radially symmetric flow profile. The transverse flow vector as a function of the spatial azimuthal angle ϕ relative to the reaction plane is

$$\vec{u}_T = (u^x, u^y) \simeq (u_T(\phi)\cos\phi, u_T(\phi)\sin\phi), \quad (4.1)$$

where in the second step we have assumed that the flow is approximately radially symmetric. The transverse flow velocity is then expanded in harmonics

$$u_T(\phi) = u_T^{(0)} + 2u_T^{(2)}\cos 2\phi + 2u_T^{(4)}\cos 4\phi + \text{other harmonics}, \quad (4.2)$$

and the thermal factor with $\vec{p} = (p_T\cos\phi_p, p_T\sin\phi_p)$ reads

$$e^{\vec{p}\cdot\vec{u}/T} \simeq e^{\frac{p_T}{T}u_T^{(0)}\cos(\phi_p-\phi)}\left[1 + \frac{2p_T}{T}u_T^{(2)}\cos 2\phi + \frac{1}{2}\left(\frac{2p_T}{T}u_T^{(2)}\cos 2\phi\right)^2 + \cdots\right], \quad (4.3)$$

$$\simeq e^{\frac{p_T}{T}u_T^{(0)}(\cos\phi_p-\phi)}\left[1 + \frac{2p_T}{T}u_T^{(2)}\cos 2\phi_p + \left(\frac{p_T}{T}u_T^{(2)}\right)^2\cos 4\phi_p + \cdots\right]. \quad (4.4)$$

The leading exponential strongly correlates coordinate space angle ϕ and the momentum space angle ϕ_p. In the second line we have anticipated the saddle point approximation, (which realizes this correlation) and set $\phi \simeq \phi_p$ in the post-exponent. The second term in square brackets determines the linear response coefficient w_2 and rises linearly with momentum, $w_2 \sim p_T u_T^{(2)}/T$. The third term determines the nonlinear response coefficient $w_{4(22)}$, and grows quadratically with momentum, $w_{4(22)} \sim \frac{1}{2}(p_T u_T^{(2)}/T)^2$. At high p_T this quadratic growth overwhelms the (neglected) linear response due to $u_T^{(4)}$, and leads to the characteristic relation $v_4 = \frac{1}{2}v_2^2$. An entirely identical argument shows that $v_5 = v_2v_3$ at high momentum in ideal hydrodynamics.

The Borghini-Ollitrault argument given above shows that the response coefficients in ideal hydro should asymptote at large momentum,

$$\frac{w_{4(22)}/\epsilon_2^2}{(w_2/\epsilon_2)^2} \xrightarrow[p_T\to\infty]{} \frac{1}{2}, \qquad \frac{w_{5(23)}/(\epsilon_2\epsilon_3)}{(w_2/\epsilon_2)(w_3/\epsilon_3)} \xrightarrow[p_T\to\infty]{} 1. \quad (4.5)$$

When fluctuations are included these asymptotic relations are modified [24]:

$$\frac{v_4\{2\}}{v_2\{2\}^2} \xrightarrow[p_T\to\infty]{} \frac{1}{2}\left(\frac{\langle\epsilon_2^4\rangle}{\langle\epsilon_2^2\rangle^2}\right)^{1/2}, \qquad \frac{v_5\{2\}}{v_2\{2\}v_3\{2\}} \xrightarrow[p_T\to\infty]{} \left(\frac{\langle(\epsilon_2\epsilon_3)^2\rangle}{\langle\epsilon_2^2\rangle\langle\epsilon_3^2\rangle}\right)^{1/2}. \quad (4.6)$$

Previous studies of v_4 in the Ψ_2 plane (see Sec. II B) have shown that such geometrical factors are essential to reproducing the centrality dependence of v_4/v_2^2 [24]. Table I records the geometrical ratios in Eq. (4.6) as a function of centrality.

We have found that rather large p_T is needed to see the nonlinear limit given by Eq. (4.6). In the current framework, the linear and nonlinear response terms, and their interference, determine the full result

$$v_4\{2\}(p_T) = \langle\langle |w_4(p_T)e^{-i4\Phi_4} + w_{4(22)}(p_T)e^{-i4\Phi_2}|^2\rangle\rangle^{1/2}. \quad (4.7)$$

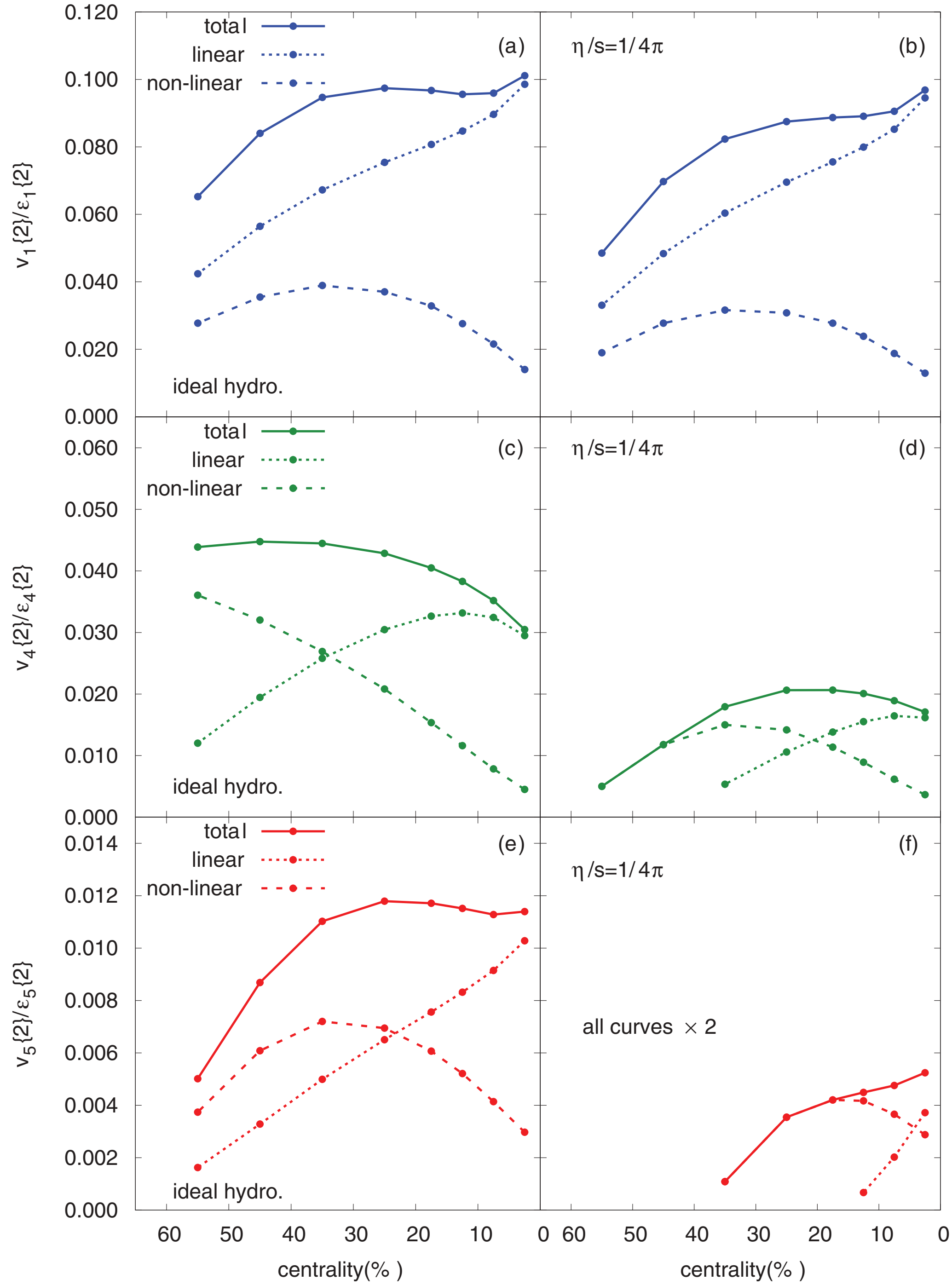

FIG. 4. (Color online) v_1, v_4, and v_5 versus centrality in ideal and viscous hydrodynamics. To keep the ideal and viscous curves on the same scale we have multiplied the viscous v_5 curves by a factor of two. In the viscous case, the linear response is neglected when the response coefficients turn negative, i.e., outside of the region of applicability of viscous hydrodynamics.

Figure 5 shows the complete result for $v_4\{2\}/v_2\{2\}^2$ (scaled by $\langle\epsilon_2^4\rangle/\langle\epsilon_2^2\rangle^2$) for ideal and viscous hydrodynamics. Focusing on the ideal results, we see that full results (the solid lines) approach the nonlinear expectation of Borghini and Ollitrault (the dashed line) only very slowly. This is in large part because $w_4(p_T)$ is only qualitatively linear at subasymptotic p_T and increases almost quadratically at intermediate $p_T \sim 1.5$ GeV, momentarily keeping up with the nonlinear response. When viscous corrections are included, the nonlinear results become dominant in peripheral collisions. Similar results for v_5 in ideal and viscous hydrodynamics are also shown in Fig. 5. In the viscous case, the nonlinear result gives almost the full $v_5\{2\}$ for all centrality classes shown.

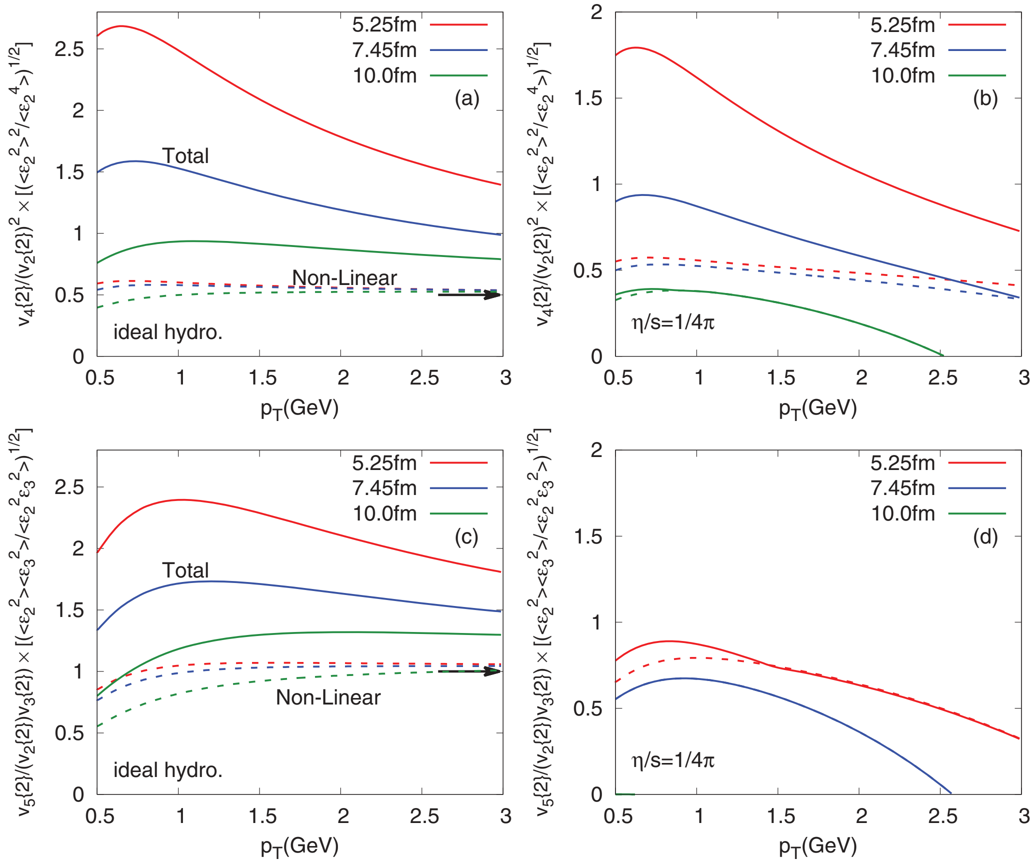

FIG. 5. (Color online) Results for v_4 and v_5 for ideal and viscous hydrodynamics at various impact parameters. The Borghini-Ollitrault expectation is indicated by the arrows for the ideal v_4 and v_5 curves [23].

It is worth noting that the magnitude of the viscous corrections as a function of p_T for v_4 and v_5 are sensitive to ansatz used for the viscous distribution function, δf [26]. In particular, the quadratic ansatz used in this work assumes that the quasiparticle energy loss is independent of momentum, $dp/dt \propto$ const. A linear ansatz for δf is better motivated for QCD-like theories and results in smaller viscous corrections for v_4 and v_5 as a function of p_T [37]. A complete discussion of this point is reserved for future work.

Figure 6 presents the corresponding analysis for $v_1(p_T)$. We see that the nonlinear terms provide a correction to the linear response which grows with p_T due to the quadratic dependence of the nonlinear response coefficients, $w_{1(23)} \propto p_T^2$. We note that the viscous corrections are approximately the same for $v_1(p_T)$ and $v_2(p_T)$, as expected from the discussion of viscous corrections given in Sec. II B.

B. Discussion

We have presented a framework of nonlinear response to understand the higher harmonics generated in heavy ion collisions. Then we extracted the nonlinear response coefficients using ideal and viscous hydrodynamics and studied the dependence on the shear viscosity, in Fig. 2. The pattern of viscous corrections is further analyzed in Fig. 3 and explained in Sec. III B. Generally, when the harmonic order is large, the nonlinear response is less damped than the corresponding linear response. Thus, when viscosity is included in hydrodynamic simulations, the nonlinear response becomes increasingly important for the higher harmonics. This qualitative reasoning is confirmed in Fig. 4 which shows v_1, v_4, and v_5 using linear and nonlinear response and is the principal result of this work. We see that the nonlinear response is essential for v_4 and v_5, and constitutes an important correction for v_1.

Experimentally, the relative contributions of the linear and nonlinear response can be disentangled by measuring v_5 in the $2\Psi_2 + 3\Psi_3$ and Ψ_5 planes, i.e., by measuring

$$v_{5(23)} \equiv \langle \cos(5\phi_{\boldsymbol{p}} - 2\Psi_2 - 3\Psi_3) \rangle \quad \text{and} \\ v_{5(5)} \equiv \langle \cos 5(\phi_{\boldsymbol{p}} - \Psi_5) \rangle \,. \tag{4.8}$$

Although a full discussion of this and similar measurements is reserved for future work, a qualitative expectation based on Figs. 4(e) and 4(f) is that the $\langle \cos(5\Psi_5 - 3\Psi_3 - 2\Psi_2) \rangle$ correlation should be strong compared to the geometric average, and should change rapidly from central to midcentral collisions. Qualitatively, this is precisely what was observed recently by the ATLAS collaboration [11].

The nonlinear response can also be studied by analyzing the p_T dependence of the flow harmonics. Figures 5 and 6 exhibit $v_4(p_T)$, $v_5(p_T)$, and $v_1(p_T)$. In ideal hydrodynamics at large p_T we expect to find $v_4 = \frac{1}{2} v_2^2$ on an event by event basis. Our nonlinear response coefficients corroborate this nonlinear

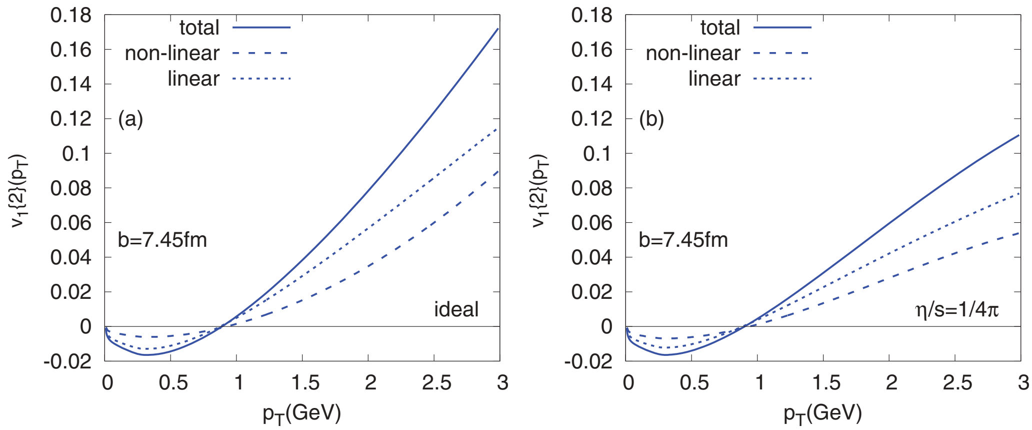

FIG. 6. (Color online) $v_1(p_T)\{2\}$ [Eq. (2.21)] in ideal and viscous hydrodynamics from the linear response to ϵ_1, the nonlinear response to $\epsilon_2\epsilon_3$, and the total response, Eq. (2.23).

expectation for v_4 and an analogous relation for v_5, $v_5 = v_2 v_3$. However, since what is normally measured is $v_4\{2\}/(v_2\{2\})^2$ and not $\langle\langle v_4/v_2^2\rangle\rangle$, this ideal nonlinear expectation must be multiplied by $(\langle\epsilon_2^4\rangle/\langle\epsilon_2^2\rangle^2)^{1/2}$ when comparing to the experimental data [24]. In addition, this expectation of ideal hydrodynamics is broken by viscous corrections, and by the linear response to the fourth order cumulant $\mathcal{C}_4$ (i.e., ϵ_4). When all of these corrections are taken into account, we find that relations such as $v_4 = \frac{1}{2}v_2^2$ and $v_5 = v_2 v_3$ provide only a rough guide to the full result.

Throughout we have assumed perfect correlation between Ψ_2 and Φ_2 and Ψ_3 and Φ_3. This strict correlation is only approximately true. For instance the combination of a v_1 and a v_3 can yield a v_2,

$$v_2 e^{-i2\Psi_2} = w_2 e^{-i2\Phi_2} + w_{2(13)} e^{-i3\Phi_3+\Phi_1}. \tag{4.9}$$

This naturally provides a correlation between the Ψ_2 and Ψ_3 plane, although the geometric correlation between Φ_2 and Φ_3 is negligibly small. Indeed the (Ψ_2, Ψ_3) correlation, which was very recently observed by the ATLAS collaboration [11], is too large to be easily explained with the geometric correlations of the Glauber model. Similarly, assuming that the linear response to ϵ_6 is negligible, one could expect that in central collisions v_6 is determined by the quadratic response to v_3, while in peripheral collisions v_6 is determined by a cubic response to v_2

$$v_6 e^{-i6\Psi_6} = w_{6(222)} e^{-i6\Phi_2} + w_{6(33)} e^{-i6\Phi_3}. \tag{4.10}$$

Qualitatively, this pattern is consistent with the observed (Ψ_6, Ψ_3) and (Ψ_6, Ψ_2) correlations presented in [11]. It will be interesting to see if all of the observed correlations can be quantitatively understood with the nonlinear response theory outlined in this paper. A full quantitative comparison with the experimental data is reserved for future work.

ACKNOWLEDGMENTS

We thank J. Y. Ollitrault, Z. Qiu, and U. Heinz for many constructive and insightful comments. D.T. is a RIKEN-RBRC fellow. This work is supported in part by the Sloan Foundation and by the Department of Energy through the Outstanding Junior Investigator program, DE-FG-02-08ER4154.

[1] Sergei A. Voloshin, Arthur M. Poskanzer, and Raimond Snellings (2008), arXiv:0809.2949 [nucl-ex]
[2] Derek A. Teaney, *Quark Gluon Plasma 4*, edited by R. C. Hwa and X. N. Wang (World Scientific, Singapore, (2009).
[3] Peter F. Kolb and Ulrich W. Heinz, *Quark Gluon Plasma 3*, edited by R. C. Hwa and X. N. Wang (World Scientific, Singapore, 2003).
[4] J. Takahashi *et al.*, Phys. Rev. Lett. **103**, 242301 (2009).
[5] Paul Sorensen, J. Phys. G **37**, 094011 (2010).
[6] G. L. Ma, S. Zhang, Y. G. Ma, H. Z. Huang, X. Z. Cai *et al.*, Phys. Lett. B **641**, 362 (2006).
[7] B. Alver and G. Roland, Phys. Rev. C **81**, 054905 (2010).
[8] Matthew Luzum, Phys. Lett. B **696**, 499 (2011).
[9] Derek Teaney and Li Yan, Phys. Rev. C **83**, 064904 (2011).
[10] Rajeev S. Bhalerao, Matthew Luzum, and Jean-Yves Ollitrault, Phys. Rev. C **84**, 034910 (2011).
[11] The ATLAS Collaboration, "Measurement of reaction plane correlations in Pb-Pb collisions at $\sqrt{s_{NN}} = 2.76$ TeV", (May 2012), ATLAS-CONF-2012-049. See also https://cdsweb.cern.ch/record/1451882.
[12] Burak Han Alver, Clement Gombeaud, Matthew Luzum, and Jean-Yves Ollitrault, Phys. Rev. C **82**, 034913 (2010).
[13] Zhi Qiu and Ulrich W. Heinz, Phys. Rev. C **84**, 024911 (2011).
[14] Fernando G. Gardim, Frederique Grassi, Matthew Luzum, and Jean-Yves Ollitrault, Phys. Rev. C **85**, 024908 (2012).
[15] Bjorn Schenke, Sangyong Jeon, and Charles Gale, Phys. Rev. Lett. **106**, 042301 (2011).
[16] Hannah Petersen, Guang-You Qin, Steffen A. Bass, and Berndt Muller, Phys. Rev. C **82**, 041901(R) (2010).
[17] Fernando G. Gardim, Frederique Grassi, Yogiro Hama, Matthew Luzum, and Jean-Yves Ollitrault, Phys. Rev. C **83**, 064901 (2011).
[18] Hannu Holopainen, Harri Niemi, and Kari J. Eskola, Phys. Rev. C **83**, 034901 (2011).
[19] K. Werner, Iu. Karpenko, T. Pierog, M. Bleicher, and K. Mikhailov, Phys. Rev. C **82**, 044904 (2010).

[20] Jean-Yves Ollitrault, Phys. Rev. D **46**, 229 (1992).
[21] Steven S. Gubser and Amos Yarom, Nucl. Phys. B **846**, 469 (2011).
[22] Peter F. Kolb, Phys. Rev. C **68**, 031902(R) (2003).
[23] Nicolas Borghini and Jean-Yves Ollitrault, Phys. Lett. B **642**, 227 (2006).
[24] Clement Gombeaud and Jean-Yves Ollitrault, Phys. Rev. C **81**, 014901 (2010).
[25] Matthew Luzum, Clement Gombeaud, and Jean-Yves Ollitrault, Phys. Rev. C **81**, 054910 (2010).
[26] Matthew Luzum and Jean-Yves Ollitrault, Phys. Rev. C **82**, 014906 (2010).
[27] Yuting Bai (STAR Collaboration), J. Phys. G **34**, S903 (2007).
[28] A. Adare *et al.* (PHENIX Collaboration), Phys. Rev. Lett. **105**, 062301 (2010).
[29] B. Alver, M. Baker, C. Loizides, and P. Steinberg (2008), arXiv:0805.4411 [nucl-ex].
[30] Rajeev S. Bhalerao, Matthew Luzum, and Jean-Yves Ollitrault, Phys. Rev. C **84**, 054901 (2011).
[31] Jiangyong Jia and Derek Teaney (2012), arXiv:1205.3585 [nucl-ex].
[32] Rudolf Baier, Paul Romatschke, Dam Thanh Son, Andrei O. Starinets, and Mikhail A. Stephanov, JHEP **0804**, 100 (2008).
[33] K. Dusling and D. Teaney, Phys. Rev. C **77**, 034905 (2008).
[34] Sayantani Bhattacharyya, Shiraz Minwalla, Veronika E. Hubeny, and Mukund Rangamani, JHEP 02 (2008) 045.
[35] Matthew Luzum and Paul Romatschke, Phys. Rev. C **78**, 034915 (2008).
[36] Derek Teaney, Phys. Rev. C **68**, 034913 (2003).
[37] Kevin Dusling, Guy D. Moore, and Derek Teaney, Phys. Rev. C **81**, 034907 (2010).
[38] Ekaterina Retinskaya, Matthew Luzum, and Jean-Yves Ollitrault, Phys. Rev. Lett. **108**, 252302 (2012).
[39] J. P. Blaizot and Jean-Yves Ollitrault, Nucl. Phys. A **458**, 745 (1986).